SCIENCE CHINA
Information Sciences

• RESEARCH PAPER •

February 2021, Vol. 64 122502:1–122502:10
https://doi.org/10.1007/s11432-020-3075-2

Generation of two-axis countertwisting squeezed spin states via Uhrig dynamical decoupling

Jiying ZHANG[1*], Shan WU[1], Yongchang ZHANG[2] & Zhengwei ZHOU[3,4*]

[1]*Institute for Interdisciplinary Research, Jianghan University, Wuhan* 430056*, China;*
[2]*Department of Physics and Astronomy, Aarhus University, Ny Munkegade* 120 DK 8000*, Denmark;*
[3]*Key Laboratory of Quantum Information, University of Science and Technology of China, Chinese Academy of Sciences, Hefei* 230026*, China;*
[4]*CAS Center for Excellence in Quantum Information and Quantum Physics, Hefei* 230026*, China*

Received 19 May 2020/Revised 29 July 2020/Accepted 3 September 2020/Published online 4 January 2021

Abstract We propose a scheme to generate two-axis countertwisting squeezed spin states from a one-axis twisting Hamiltonian via Uhrig dynamical decoupling. The proposed scheme significantly reduces the number of control pulses or requires shorter evolution time compared to previous proposals. The minimum number of applied pulses changes relative to the spin number almost linearly. The proposed scheme significantly relieves the experimental demand on the applied pulses or the evolution time, and we expect it would be within the reach of current spin squeezing experiment.

Keywords squeezed spin states, Uhrig dynamical decoupling, control pulses, quantum control, quantum metrology, quantum information science

Citation Zhang J Y, Wu S, Zhang Y C, et al. Generation of two-axis countertwisting squeezed spin states via Uhrig dynamical decoupling. Sci China Inf Sci, 2021, 64(2): 122502, https://doi.org/10.1007/s11432-020-3075-2

1 Introduction

Squeezed spin states (SSS) [1–4] are a type of quantum correlated states of a spin ensemble. SSS can reduce fluctuations in one of the collective spin components and, therefore, play a crucial role in quantum metrology [2,3,5–11] and quantum information science [12–24]. Kitagawa and Ueda identified two types of SSS: one-axis twisting (OAT) and two-axis countertwisting (TACT) [1]. OAT SSS can be realized by the Hamiltonian $H_1 \propto J_x^2$ and allow precise measurements to scale with $1/N^{2/3}$, where N is the spin number of the system. TACT can be generated under the Hamiltonian $H_2 \propto J_x^2 - J_y^2$ and causes Heisenberg limited noise reduction to scale as $1/N$. The squeezing direction of OAT is time-dependent while that of TACT is fixed. Thus, TACT provides better spin squeezing than OAT.

OAT SSS have been achieved experimentally in binary Bose-Einstein condensates (BEC), where the OAT Hamiltonian inherently turns up from inter- and intra-component interactions. A natural promotion for preparing SSS is to achieve the high quality of the OAT and even to realize the TACT. Coherent control of external pulses is an effective way to improve an OAT SSS, and to date, various related schemes have been proposed [25–30]. In a previous scheme [26], one or two global rotation pulses with an appropriate evolution time and optimized rotation angles can achieve significant improvement compared to OAT squeezing. However, to achieve the best squeezing, this scheme requires a long evolution time, which would be an obstacle in systems with a short coherence time. In addition, that scheme is spin-number-dependent; thus, it is naturally difficult to apply to some systems, such as ultracold atomic gases, where the exact spin number N is unknown. Another scheme [25], stroboscopically applied a large number of repeated Rabi pulses and successfully converted the OAT to TACT. However, in that scheme, the large number of pulses acting on the atoms inevitably results in accumulated noise and imperfect control pulses. Some subsequent studies [27,28] developed this idea, and reduced the applied pulse number to a much smaller value; however, it is still difficult to realize them in experiment.

* Corresponding author (email: jyzhang04@jhun.edu.cn, zwzhou@ustc.edu.cn)

In this paper, we propose a scheme to generate TACT SSS by manipulating the OAT interactions via Uhrig dynamical decoupling (UDD) [31–33]. Taking advantage of the optimal control on external pulse sequences provided by UDD, we found that only a small number of pulses are required to realize TACT. Compared to previous schemes that require 2000 [25] and 100 [27] control pulses to reach the TACT type of spin squeezing, the proposed scheme requires only 38 control pulses. This dramatic reduction of manipulated resources sheds light on the experimental realization of TACT SSS [34].

This remainder of this paper is organized as follows. In Section 2, we present the theoretical scheme based on UDD and show the specific pulse sequence. In Section 3, we provide numerical results and compare the new UDD scheme to our previous proposal based on Trotter-Suzuki expansion theory [27]. Conclusion and suggestion for future work are presented in Section 4.

2 The scheme

We consider a two-component BEC consisting of N atoms in two different hyperfine states $|g\rangle$ and $|e\rangle$ coupled by an external field (microwave field or a Raman laser). Under the resonant condition, the Hamiltonian of this system is [35, 36]

$$H_1 = H_g + H_e + H_{\text{ext}}, \tag{1}$$

where H_g and H_e describe the two-component condensate and H_{ext} is the interaction with the external field. In the second quantization, the above terms are given by($\hbar = 1$) [35, 36]

$$\begin{aligned} H_i &= \int \mathrm{d}^3\boldsymbol{r}\Psi_i^\dagger(\boldsymbol{r})\left[-\frac{\nabla^2}{2m} + V_i(\boldsymbol{r}) + \sum_{j=g,e}\frac{U_{ij}}{2}\Psi_j^\dagger(\boldsymbol{r})\Psi_j(\boldsymbol{r})\right]\Psi_i(\boldsymbol{r}), \quad i = g, e, \\ H_{\text{ext}} &= \frac{1}{2}\int \mathrm{d}^3\boldsymbol{r}\left[\Lambda(t)\Psi_g^\dagger(\boldsymbol{r})\Psi_e(\boldsymbol{r}) + \Lambda(t)^*\Psi_e^\dagger(\boldsymbol{r})\Psi_g(\boldsymbol{r})\right], \end{aligned} \tag{2}$$

where $\Psi_i(\boldsymbol{r})$ and $\Psi_i^\dagger(\boldsymbol{r})$ are the atomic field operators that annihilate and create a particle at position $\boldsymbol{r}$ in the hyperfine state $|i\rangle$ $(i = g, e)$. The trapping potential for atoms in state $|g\rangle$ and $|e\rangle$ is presented by $V_g(\boldsymbol{r})$ and $V_e(\boldsymbol{r})$, and the mass of the atoms is m. The interaction strengths are denoted by U_{gg}, U_{ee} and U_{ge} for collisions between particles in state $|g\rangle$, $|e\rangle$ and interspecies collisions, respectively. $\Lambda(t)$ is the effective Rabi frequency.

We assume that the spatial degrees of freedom can be described using one spatial mode function for each component $\Psi_g(\boldsymbol{r}) = a\varphi_g(\boldsymbol{r})$ and $\Psi_e(\boldsymbol{r}) = b\varphi_e(\boldsymbol{r})$, where $\varphi_g(\boldsymbol{r})$ and $\varphi_e(\boldsymbol{r})$ are normalized wave functions, and a and b are bosonic annihilation operators in the internal state $|g\rangle$ and $|e\rangle$ obeying the usual bosonic commutation relations $[a, a^\dagger] = 1$, $[b, b^\dagger] = 1$, $[a, b] = 0$ and $[a, b^\dagger] = 0$. Under the single-mode approximation, the Hamiltonian in (1) can be rewritten as

$$H_1 = \omega_g a^\dagger a + \omega_e b^\dagger b + \frac{\Omega(t)}{2}(a^\dagger b + a b^\dagger) + u_{ge}a^\dagger a b^\dagger b + \frac{u_{gg}}{2}a^{\dagger 2}a^2 + \frac{u_{ee}}{2}b^{\dagger 2}b^2, \tag{3}$$

where the relevant parameters are as follows:

$$\omega_{g(e)} = \int \mathrm{d}^3\boldsymbol{r}\varphi_{g(e)}^*(\boldsymbol{r})\left[-\frac{\nabla^2}{2m} + V_{g(e)}(\boldsymbol{r})\right]\varphi_{g(e)}(\boldsymbol{r}), \tag{4}$$

$$u_{\alpha\beta} = U_{\alpha\beta}\int \mathrm{d}^3\boldsymbol{r}|\varphi_\alpha(\boldsymbol{r})|^2|\varphi_\beta(\boldsymbol{r})|^2, \quad \alpha, \beta = g, e, \tag{5}$$

$$\Omega(t) = \Lambda(t)\int \mathrm{d}^3\boldsymbol{r}\varphi_g^*(\boldsymbol{r})\varphi_e(\boldsymbol{r}). \tag{6}$$

We define the angular-momentum operators in term of the BEC operators in this way: $J_x = \frac{i}{2}(b^\dagger a - a^\dagger b)$, $J_y = \frac{1}{2}(a^\dagger b + b^\dagger a)$ and $J_z = \frac{1}{2}(a^\dagger a - b^\dagger b)$, the Hamiltonian of the two-component BEC shown by (3) reduces to the OAT Hamiltonian:

$$H_1 = \chi J_z^2 + \Omega(t)J_y + \delta J_z, \tag{7}$$

where the relevant parameters are given by

$$\chi = (u_{gg} + u_{ee} - 2u_{ge})/2, \tag{8}$$

$$\delta = \omega_g - \omega_e + (u_{gg} - u_{ee})(N-1)/2, \tag{9}$$

where χ is the effective nonlinearity resulting from intra- and interspecies interaction, and we may take $\delta = 0$.

For ideal pulses, i.e., $\chi N \ll |\Omega(t)|$, the nonlinear interaction can be ignored when the control pulses are switched on. A $\pi/2$ pulse corresponds to $\int_{-\infty}^{\infty}\Omega(t)\mathrm{d}t = \pi/2$, which can generate $\mathrm{e}^{-\mathrm{i}\chi J_x^2 t}$ and $\mathrm{e}^{-\mathrm{i}\chi(-J_y^2)\Delta t}$ from $\mathrm{e}^{-\mathrm{i}\chi J_z^2 t}$ via

$$R^y_{-\frac{\pi}{2}}\mathrm{e}^{-\mathrm{i}\chi J_z^2 t}R^y_{\frac{\pi}{2}} = \mathrm{e}^{-\mathrm{i}\chi J_x^2 t}, \tag{10}$$

$$R^y_{-\frac{\pi}{2}}\mathrm{e}^{-\mathrm{i}\chi J_z^2\frac{\Delta t}{2}}R^y_{\frac{\pi}{2}}\mathrm{e}^{-\mathrm{i}\chi J_z^2\Delta t}R^y_{-\frac{\pi}{2}}\mathrm{e}^{-\mathrm{i}\chi J_z^2\frac{\Delta t}{2}}R^y_{\frac{\pi}{2}} \simeq \mathrm{e}^{-\mathrm{i}\chi(-J_y^2)\Delta t}, \tag{11}$$

where Δt is a small time duration, and $R^y_{\pm\frac{\pi}{2}} = \mathrm{e}^{-\mathrm{i}\pm\frac{\pi}{2}J_y}$, rotating the spin around y-axis by an angle $\pm\frac{\pi}{2}$. The derivation of (11) can be described as follows.

If we assume the time evolution operator U_1 as follows:

$$\begin{aligned} U_1 &= R^y_{-\frac{\pi}{2}}\mathrm{e}^{-\mathrm{i}\chi J_z^2\frac{\Delta t}{2}}R^y_{\frac{\pi}{2}}\mathrm{e}^{-\mathrm{i}\chi J_z^2\Delta t}R^y_{-\frac{\pi}{2}}\mathrm{e}^{-\mathrm{i}\chi J_z^2\frac{\Delta t}{2}}R^y_{\frac{\pi}{2}} \\ &= \mathrm{e}^{-\mathrm{i}\chi J_x^2\frac{\Delta t}{2}}\mathrm{e}^{-\mathrm{i}\chi J_z^2\Delta t}\mathrm{e}^{-\mathrm{i}\chi J_x^2\frac{\Delta t}{2}} \\ &= \mathrm{e}^{-\mathrm{i}\chi J_x^2\frac{\Delta t}{2}}\mathrm{e}^{-\mathrm{i}\chi J_z^2\frac{\Delta t}{2}}\mathrm{e}^{-\mathrm{i}\chi J_z^2\frac{\Delta t}{2}}\mathrm{e}^{-\mathrm{i}\chi J_x^2\frac{\Delta t}{2}}. \end{aligned} \tag{12}$$

Using the Baker-Campbell-Hausdorff (BCH) formula, the evolution operator U_1 becomes

$$U_1 = \exp\left(-\mathrm{i}\chi(J_x^2+J_z^2)\Delta t - \frac{(\chi\Delta t)^3}{24}(2[J_z^2,\{J_x,\{J_y,J_z\}\}] + [J_x^2,\{J_x,\{J_y,J_z\}\}]) + O((\chi\Delta t)^3)\right), \tag{13}$$

where $\{A,B\} = AB + BA$ denotes the anticommutator of operator A and B. For small $\chi\Delta t$, we have $-\frac{(\chi\Delta t)^3}{24}(2[J_z^2,\{J_x,\{J_y,J_z\}\}] + [J_x^2,\{J_x,\{J_y,J_z\}\}]) + O((\Delta t)^3) \simeq 0$ after ignoring the 3rd- and higher-order terms. Because of the commutation relation $[J^2, H_1] = 0$, $J^2 = J_x^2 + J_y^2 + J_z^2$ is conserved during the dynamics. So up to a constant phase factor, the evolution operator can be rewritten as

$$\begin{aligned} U_1 &\simeq \mathrm{e}^{-\mathrm{i}\chi(J_x^2+J_z^2)\Delta t} \\ &= \mathrm{e}^{-\mathrm{i}\chi(J_x^2+J_z^2+J_y^2-J_y^2)\Delta t} \\ &= \mathrm{e}^{-\mathrm{i}\chi(-J_y^2)\Delta t}. \end{aligned} \tag{14}$$

Hence, according to (12)–(14), one can obtain the relation of (11).

It is well known that UDD can eliminate the qubit-bath coupling to the Mth-order of the whole evolution time t_w using M instantaneous π pulses applied at [31,32]

$$t_j = t_w \sin^2\frac{j\pi}{2(M+1)}, \quad j = 1,2,\ldots,M. \tag{15}$$

Inspired by the main idea of UDD that the system-environment interaction H_{SB} is switched between H_{SB} and $-H_{SB}$ by external pulses applied at t_j and UDD may get the best result in the sense that it uses the minimum number of control pulses for a given order of decoupling in dynamical decoupling field, we propose to generate TACT from OAT based on UDD. Since the desired TACT Hamiltonian is $H_2 \propto \chi(J_x^2 - J_y^2)$, we arrange the spins to evolve alternately under the Hamiltonian χJ_x^2 and $-\chi J_y^2$ following the pulse sequence of UDD. Hereafter we abbreviate the M-pulse UDD as UDD_M, and the corresponding sequence of χJ_x^2 and $-\chi J_y^2$ to get TACT is written as UDD_M^J. The schematic plots of UDD_M^J with $M = 1,2,\ldots,6$ are shown in Figure 1(a). We apply the pulse sequence according to UDD_M^J for each single period $t_w = t_{\mathrm{opt}}/N_c$, where t_{opt} is the optimal squeezing time when the spin squeezing reaches its minimum, and N_c is the total number of cycles. The entire pulse sequence is named as $\mathrm{PS}_{\mathrm{UDD}_M^J}$ as shown in Figure 1(b).

Based on UDD_M^J, let us turn to the realistic pulse sequence, namely UDD_M^T, that is applied to generate the corresponding effective interactions of χJ_x^2 and $-\chi J_y^2$ from the system Hamiltonian $H_1 = \chi J_z^2 + \Omega(t)J_y$ respectively according to (10) and (11) as illustrated in Figure 2(a). The red and green rectangles

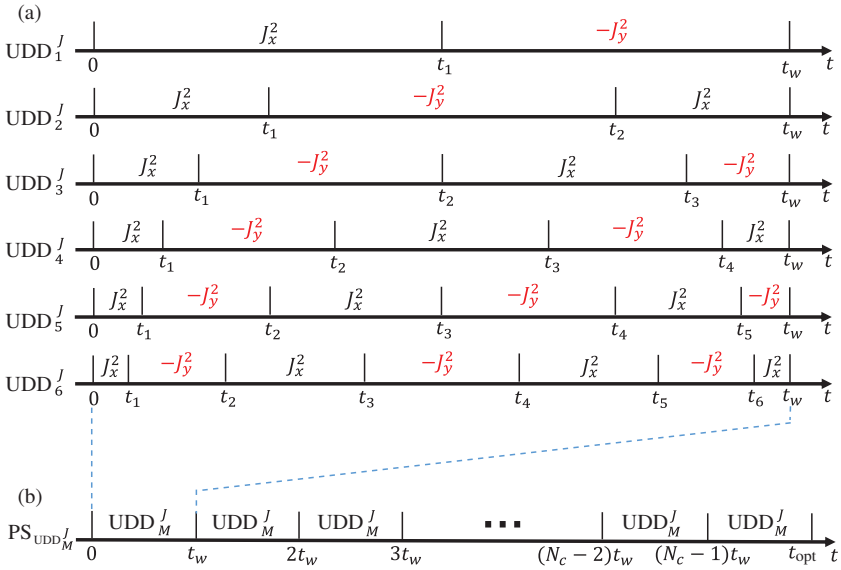

Figure 1 (Color online) Schematic illustrations of the alternate evolution under the Hamiltonian χJ_x^2 and $-\chi J_y^2$ according to UDD. (a) The sequence of χJ_x^2 and $-\chi J_y^2$ corresponding to UDD_M^J for $M = 1, 2, \ldots, 6$, and for simplicity χ is omitted. (b) $\mathrm{PS}_{\mathrm{UDD}_M^J}$, the whole series of χJ_x^2 and $-\chi J_y^2$ from $t = 0$ to $t = t_{\mathrm{opt}}$.

represent the $\frac{\pi}{2}$ and $-\frac{\pi}{2}$ pulses around y-axis respectively, between which the system evolves under the Hamiltonian $H_1 = \chi J_z^2$. For UDD_{M-1}^T and UDD_M^T with M being even, the $\pm\frac{\pi}{2}$ pulse is instantly applied at the following time:

$$\begin{cases} T_0 = 0, \\ T_m = \dfrac{3t_m - t_{m+1}}{2} + \displaystyle\sum_{i=1}^{\frac{m}{2}} t_{2i} - \sum_{i=1}^{\frac{m}{2}} t_{2i-1}, \\ T_{m+1} = T_m + t_{m+1} - t_m, \ m = 1, 3, \ldots, M-1, \\ T_w = T_{M+1} = 1 + \displaystyle\sum_{i=1}^{\frac{M}{2}} t_{2i} - \sum_{i=1}^{\frac{M}{2}} t_{2i-1}, \end{cases} \tag{16}$$

where $t_M = 1$ for UDD_{M-1}^T.

Being subject to the impact of the UDD_M^T pulse sequence, the atomic dynamics can be described by the following evolution operator:

$$\begin{aligned} U_2 = {} & \mathrm{e}^{-\mathrm{i}\chi J_x^2 (T_w - T_M)} \mathrm{e}^{-\mathrm{i}\chi J_z^2 (T_M - T_{M-1})} \\ & \cdot \mathrm{e}^{-\mathrm{i}\chi J_x^2 (T_{M-1} - T_{M-2})} \cdots \mathrm{e}^{-\mathrm{i}\chi J_x^2 (T_3 - T_2)} \\ & \cdot \mathrm{e}^{-\mathrm{i}\chi J_z^2 (T_2 - T_1)} \mathrm{e}^{-\mathrm{i}\chi J_x^2 T_1} \\ \simeq {} & \mathrm{e}^{-\mathrm{i}\frac{\chi}{3}(J_x^2 - J_y^2) T_w}. \end{aligned} \tag{17}$$

By periodically repeating the above UDD_M^T pulse sequence, we get the whole pulse sequence $\mathrm{PS}_{\mathrm{UDD}_M^T}$. Eventually the entire evolution within a duration $t_{\mathrm{opt}} = N_c T_w$, can be expressed as

$$U = U_2^{N_c} \simeq \mathrm{e}^{-\mathrm{i}\frac{\chi}{3}(J_x^2 - J_y^2) N_c T_w} = \mathrm{e}^{-\mathrm{i}\frac{\chi}{3}(J_x^2 - J_y^2) t}, \tag{18}$$

which manifests that the evolution is governed by the desired TACT Hamiltonian:

$$H_2 = \frac{\chi}{3}(J_x^2 - J_y^2) \tag{19}$$

with a reduced interaction strength $\chi/3$.

Moreover, from Figure 2 one can note that, for even M, $\mathrm{PS}_{\mathrm{UDD}_M^T}$ and $\mathrm{PS}_{\mathrm{UDD}_{M-1}^T}$ need the same pulse number $MN_c + 2$ for N_c pulse cycles. The accuracy of the former is 1-order higher than that of the

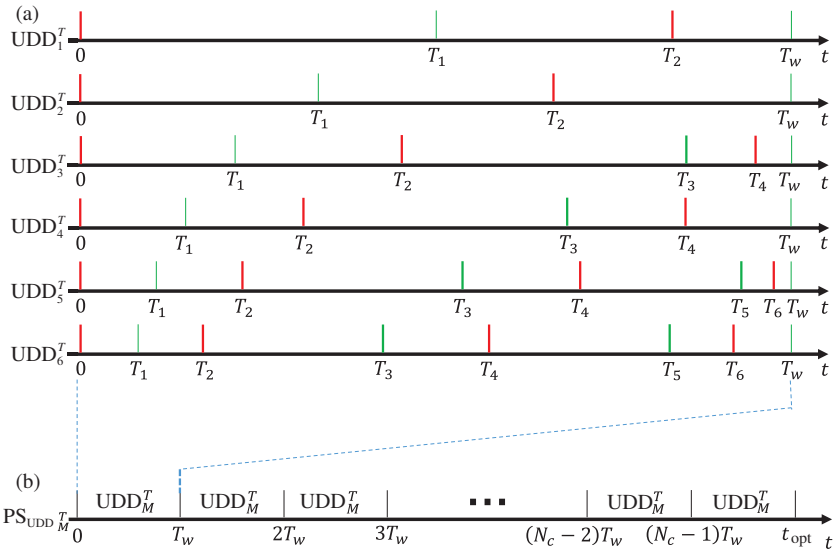

Figure 2 (Color online) An illustration of the pulse sequences for generating TACT-type Hamiltonian $H_2 \propto \chi(J_x^2 - J_y^2)$. (a) The pulse sequence of UDD_M^T for $M = 1, 2, \ldots, 6$, here the red and green rectangles correspond to the $\frac{\pi}{2}$ and $-\frac{\pi}{2}$ pulses around y axis, respectively. (b) $\mathrm{PS}_{\mathrm{UDD}_M^T}$, the whole pulse sequence from $t = 0$ to $t = t_{\mathrm{opt}}$.

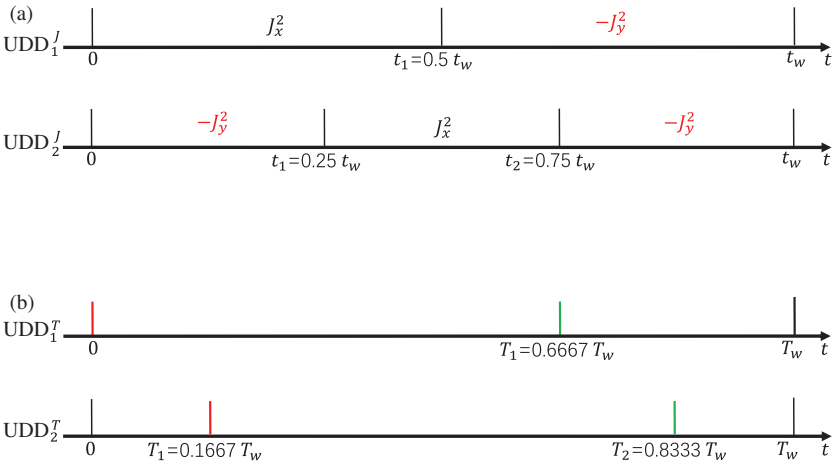

Figure 3 (Color online) (a) The sequences of χJ_x^2 and $-\chi J_y^2$ based on UDD_1^J and UDD_2^J. (b) The pulse sequences for one single period used in [25] and in our previous work [27], which can be obtained via UDD_1^J and UDD_2^J respectively.

latter. In order to achieve higher performance with smaller number of pulses, in practice, we will focus on $\mathrm{PS}_{\mathrm{UDD}_M^T}$ with $M = 2, 4, 6, \ldots$.

In addition, it should be noted that our UDD_M^T proposal is not exceptional, but actually a universal scheme in the context of pulse-assisted TACT spin squeezing. It can recover the previous schemes proposed by Liu et al. [25] and by our group [27]. According to UDD_1^J and UDD_2^J (see Figure 3(a)), one can take advantage of (10) and the following (20) to realize the free evolution of the effective Hamiltonian χJ_x^2 and $-\chi J_y^2$,

$$\begin{aligned} U_3 &= R_{-\frac{\pi}{2}} \mathrm{e}^{-\mathrm{i}\chi J_z^2 \Delta t} R_{\frac{\pi}{2}} \mathrm{e}^{-\mathrm{i}\chi J_z^2 \Delta t} \\ &= \mathrm{e}^{-\mathrm{i}\chi J_x^2 \Delta t} \mathrm{e}^{-\mathrm{i}\chi J_z^2 \Delta t} \\ &= \mathrm{e}^{-\mathrm{i}\chi(J_x^2 + J_z^2)\Delta t + \frac{i(\chi\Delta t)^2}{2}\{J_x, \{J_y, J_z\}\} + O((\chi\Delta t)^2))} \\ &\simeq \mathrm{e}^{-\mathrm{i}\chi(-J_y^2)\Delta t}, \end{aligned} \tag{20}$$

so the final realistic pulse sequence for one single period in [25] and our previous work [27] are shown in Figure 3(b).

Moreover, one can note that Liu et al.'s scheme actually corresponds to the UDD_1^J with the 1st-order approximation of the BCH formula, and our previous scheme (the TS2 scheme), which is based on Trotter-Suzuki 2nd-order expansion theory, corresponds to the UDD_2^J with the 1st-order BCH approximation, while our present UDD_M^T is the UDD_M^J $(M = 2, 4, \ldots, 6)$ with the 2nd-order approximation of the BCH formula. This is the key point that our current $\mathrm{PS}_{\mathrm{UDD}_M^T}$ scheme can reach high precision TACT with significantly smaller number of pulses, which will be discussed in detail in Section 3.

3 The numerical results and analysis

The degree of spin squeezing, following Kitagawa and Ueda's criteria, can be quantified by the squeezing parameter $\xi^2 = \frac{2(\triangle J_\perp)^2_{\min}}{J}$, where $(\triangle J_\perp)^2_{\min}$ is the smallest variance in the direction normal to the mean spin vector and $J = N/2$ is the total spin of the system. If $\xi^2 < 1$, the states are in SSS, and the states are coherent spin states when $\xi^2 = 1$. To generate the TACT Hamiltonian $H_2 \propto \chi(J_x^2 - J_y^2)$, we choose $|j, j\rangle = |\uparrow\rangle^{\otimes N}$ (all the spins are polarized along the z-axis) as the initial state.

To simulate the effective dynamics under the effective TACT Hamiltonian H_2 and the actual dynamics ruled by the Hamiltonian H_1 with the $\mathrm{PS}_{\mathrm{UDD}_M^T}$ pulse sequence, we expand the state vector evolved from the initial state $|j, j\rangle$,

$$\begin{aligned} |\psi_{\mathrm{eff}}(t)\rangle &= \mathrm{e}^{-\mathrm{i}\chi t(J_x^2 - J_y^2)/3}|j, j\rangle = \sum_m c_m(t)|j, m\rangle, \\ |\psi_{\mathrm{act}}(t)\rangle &= U_{\mathrm{PS}_{\mathrm{UDD}_M^T}}|j, j\rangle = \sum_m d_m(t)|j, m\rangle \end{aligned} \tag{21}$$

into $|j, m\rangle$, which is the common eigenstate of J^2 and J_z. Because $[J^2, H_1] = 0$ is satisfied, J^2 is conserved during the dynamics and the value of $j = N/2$ is fixed through the entire evolution. Since $m = -j, -j+1, -j+2, \ldots, j$, the dimension of the Hilbert space is $N + 1$, much smaller than 2^N, therefore, a classical computer has the capability to perform the simulation.

In the following, we demonstrate the performance of our $\mathrm{PS}_{\mathrm{UDD}_M^T}$ scheme by simulating the dynamical process numerically. To compare the $\mathrm{PS}_{\mathrm{UDD}_M^T}$ scheme with our previous TS2 proposal, we consider the system with the atom number $N = 1250$.

As demonstrated in Section 2, our $\mathrm{PS}_{\mathrm{UDD}_M^T}$ scheme results in an effective TACT Hamiltonian H_2 shown in (19) with the interaction strength $\chi_{\mathrm{eff}} = \frac{\chi}{3}$. The optimal time for generating TACT SSS using our $\mathrm{PS}_{\mathrm{UDD}_M^T}$ scheme is $\chi_{\mathrm{eff}} t_{\mathrm{opt}} \simeq 3\ln(4N)/2N$ [25]. t_{opt} is fixed for $N = 1250$ and divided into N_c cycles in $\mathrm{PS}_{\mathrm{UDD}_M^T}$, and thus the time duration for one single cycle is $T_w = \frac{t_{\mathrm{opt}}}{N_c} \simeq \frac{9\ln(4N)}{2N\chi N_c}$. Apparently T_w is N_c-dependent. UDD_M^T pulse sequence is applied in each cycle. Since UDD can reduce the error up to the M-th order of the evolution time t_w using M instant pulses, on one hand, the performance of UDD_M^T can be improved by increasing M for the same T_w (i.e., the same N_c); on the other hand, we can also improve the result of UDD_M^T via shortening T_w (i.e., increasing N_c) while keeping M unchanged.

These two behaviors have been confirmed by our numerical simulation as shown in Figure 4. The squeezing parameter ξ^2 decreases further and further with the increase of M in our $\mathrm{PS}_{\mathrm{UDD}_M^T}$ scheme for the same cycle number N_c and the dynamics of $\mathrm{PS}_{\mathrm{UDD}_M^T}$ gradually approaches the ideal dynamics controlled by the effective TACT Hamiltonian H_2. Besides, for the fixed M, the larger cycle number N_c will lead to the better squeezing performance.

To reach the TACT SSS with a high accuracy, our previous TS2 scheme demands $N_c = 50$ cycles, i.e., $N_p = 100$ control pulses in total, as shown in Figure 5. In contrast, to gain the same performance, the number of control pulses can be reduced to $N_p = 72$ ($N_c = 35$) by $\mathrm{PS}_{\mathrm{UDD}_2^T}$. Furthermore, one can note that both the pulse sequences of TS2 and $\mathrm{PS}_{\mathrm{UDD}_2^T}$ scheme in one single period stem from UDD_2^J, while the only difference between them is how they get the evolution controlled by $-J_y^2$. TS2 scheme generates $\mathrm{e}^{-\mathrm{i}\chi(-J_y^2)\Delta t}$ based on the BCH 1st-order approximation (see Eq. (20)) while $\mathrm{PS}_{\mathrm{UDD}_2^T}$ obtains $\mathrm{e}^{-\mathrm{i}\chi(-J_y^2)\Delta t}$ under the BCH 2nd-order approximation (see Eq. (11)). Hence the reduction of applied pulses number from 100 to 72 attributes to the higher-order BCH approximation adopted in the design of the pulse sequences.

Proceeding to our $\mathrm{PS}_{\mathrm{UDD}_4^T}$ scheme, we find a further reduction to $N_p = 38$ ($N_c = 9$) pulses that can achieve the same TACT SSS generated by TS2 scheme with $N_p = 100$ ($N_c = 50$) (see Figure 5). This

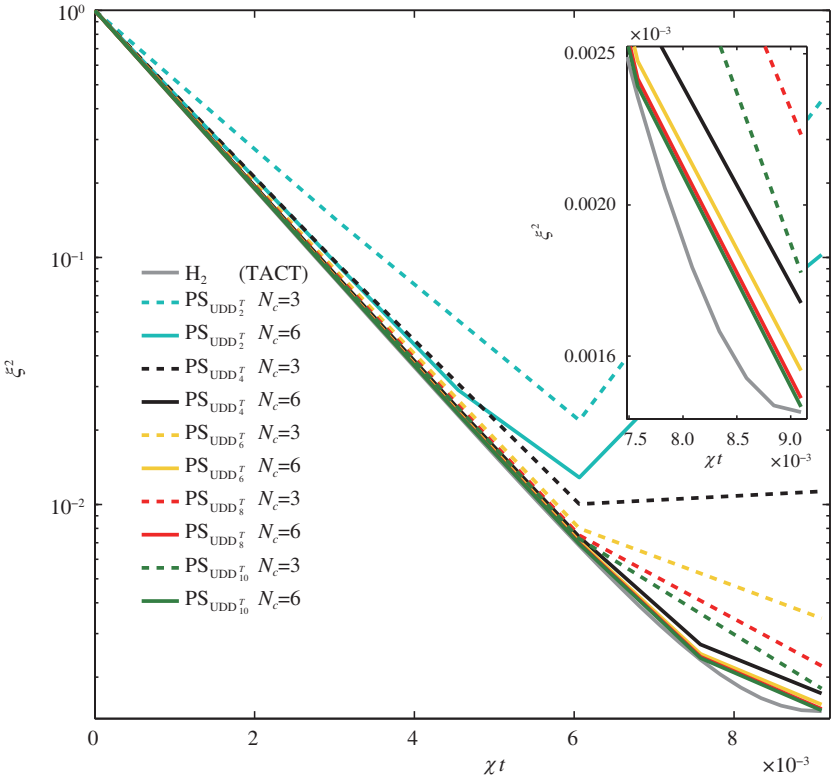

Figure 4 (Color online) The spin squeezing vs. the evolution time of our $\mathrm{PS}_{\mathrm{UDD}_M^T}$ scheme while $M = 2, 4, 6, 8, 10$ for the system with $N = 1250$ spins. The solid grey, the dotted (solid) cyan, the dotted (solid) black, the dotted (solid) yellow, the dotted (solid) red and the dotted (solid) green line display the result for the ideal TACT Hamiltonian H_2, $\mathrm{PS}_{\mathrm{UDD}_2^T}$ with $N_c = 3\,(6)$, $\mathrm{PS}_{\mathrm{UDD}_4^T}$ with $N_c = 3\,(6)$, $\mathrm{PS}_{\mathrm{UDD}_6^T}$ with $N_c = 3\,(6)$, $\mathrm{PS}_{\mathrm{UDD}_8^T}$ with $N_c = 3\,(6)$, and $\mathrm{PS}_{\mathrm{UDD}_{10}^T}$ with $N_c = 3\,(6)$, respectively. N_c is the cycle number of the pulse sequences.

improvement results from that $\mathrm{PS}_{\mathrm{UDD}_4^T}$ is based on UDD_4^J while TS2 scheme corresponds to UDD_2^J, in addition to that the BCH 2nd-order approximation is taken in $\mathrm{PS}_{\mathrm{UDD}_4^T}$ while TS2 scheme takes the 1st-order BCH approximation.

However, the total required pulse number turns up to increase for $\mathrm{PS}_{\mathrm{UDD}_M^T}$ with $M > 4$ in comparison with the result of $\mathrm{PS}_{\mathrm{UDD}_4^T}$ scheme. For example, $\mathrm{PS}_{\mathrm{UDD}_6^T}$ needs $N_p = 44$ ($N_c = 7$) control pulses as shown in Figure 5.

This implies $\mathrm{PS}_{\mathrm{UDD}_4^T}$ scheme has the best performance in the sense of employing the least number of control pulses to achieve the effective TACT Hamiltonian H_2. To confirm this conclusion, we show the numerical result of the relative error

$$E_r = \frac{\xi^2_{\mathrm{TS2}(\mathrm{PS}_{\mathrm{UDD}_M^T})} - \xi^2_{\mathrm{eff}}}{\xi^2_{\mathrm{eff}}}$$

in Figure 6. One can note that, with limited pulse numbers as discussed before, the $\mathrm{PS}_{\mathrm{UDD}_4^T}$ ($N_c = 9$) attains the smallest relative error. Though the relative error can be reduced further by increasing the order of the UDD expansion M or the cycle number (e.g., see the solid yellow line), the applied total number of pulses would, however, go beyond that of $\mathrm{PS}_{\mathrm{UDD}_4^T}$ (i.e., 38). Therefore, the analysis of relative error brings to the same conclusion; i.e., $\mathrm{PS}_{\mathrm{UDD}_4^T}$ is the optimal sequence that can minimize the number of the required pulse number.

For a given small enough accuracy, why $\mathrm{PS}_{\mathrm{UDD}_4^T}$ performs better than $\mathrm{PS}_{\mathrm{UDD}_M^T}$ with larger M for the system with $N = 1250$ spins? Taking $\mathrm{PS}_{\mathrm{UDD}_4^T}$ and $\mathrm{PS}_{\mathrm{UDD}_6^T}$ as an example, the pulse cycle number is $N_c = 9$ and $N_c = 6$ for $\mathrm{PS}_{\mathrm{UDD}_4^T}$ and $\mathrm{PS}_{\mathrm{UDD}_6^T}$ respectively which leads to the same pulse number of $N_p = 38$. Since the time duration in one cycle is $T_w \simeq \frac{9\ln(4N)}{2N\chi N_c}$, we have $T_w^{\mathrm{UDD}_4^T} \simeq \frac{9\ln(4N)}{2N\chi\times 9} < T_w^{\mathrm{UDD}_6^T} \simeq \frac{9\ln(4N)}{2N\chi\times 6}$. And this relationship leads to smaller cumulative error of $\mathrm{PS}_{\mathrm{UDD}_4^T}$ than that of $\mathrm{PS}_{\mathrm{UDD}_6^T}$. If reducing $T_w^{\mathrm{UDD}_6^T}$ by increasing the cycle number to $N_c = 7$ ($N_p = 44$), we find the spin squeezing of $\mathrm{PS}_{\mathrm{UDD}_6^T}$

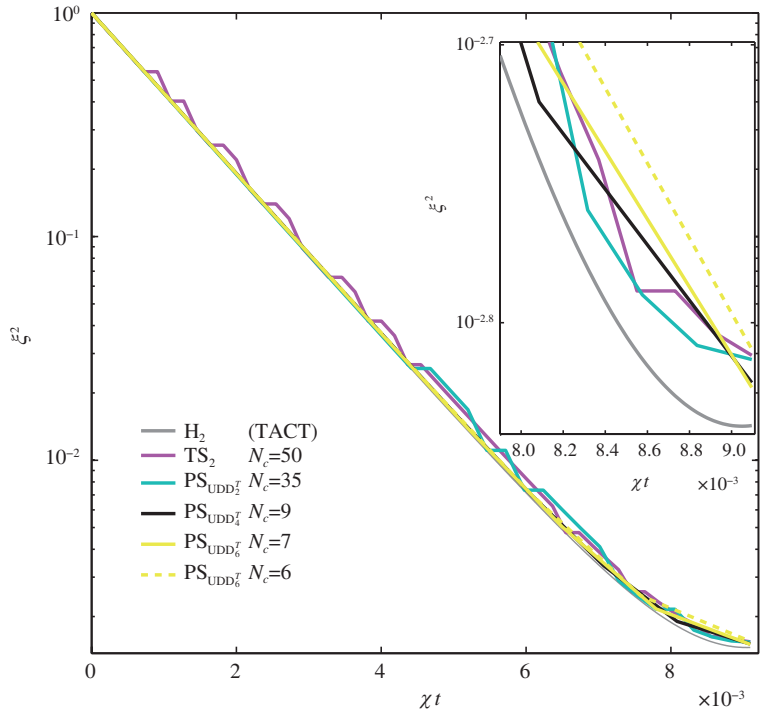

Figure 5 (Color online) The spin squeezing vs. the evolution time for $N = 1250$. The solid grey, magenta, cyan, black and yellow line and the dotted yellow line denote the result of the ideal TACT Hamiltonian H_2, the TS2 scheme with $N_c = 50$, $\mathrm{PS}_{\mathrm{UDD}_2^T}$ with $N_c = 35$, $\mathrm{PS}_{\mathrm{UDD}_4^T}$ with $N_c = 9$, and $\mathrm{PS}_{\mathrm{UDD}_6^T}$ with $N_c = 7$ and $N_c = 6$, respectively. N_c is the cycle number of the pulse sequences. A zoom-in around the optimal squeezing time is shown in the inset.

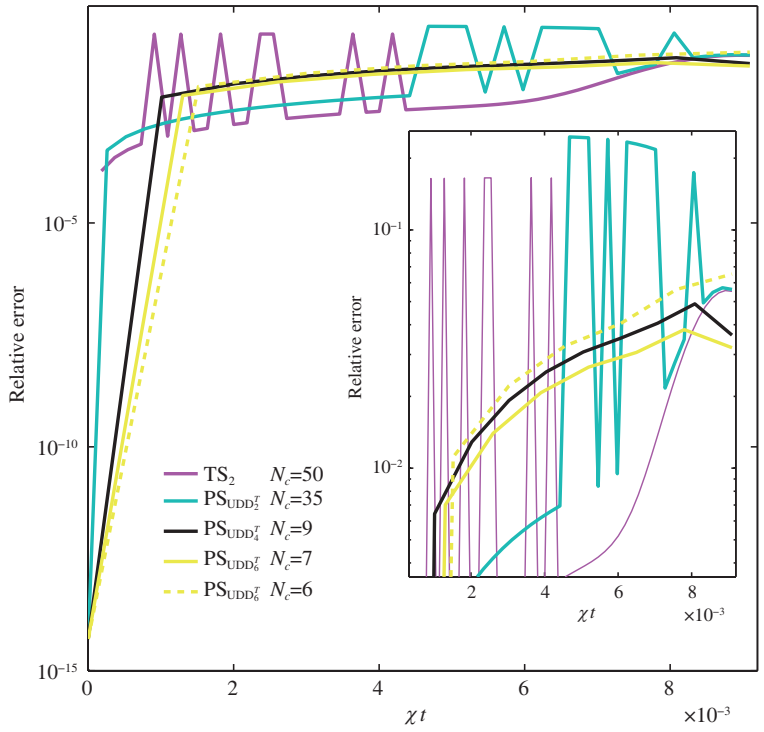

Figure 6 (Color online) The variation of the relative error $E_r = \dfrac{\xi^2_{\mathrm{TS2}(\mathrm{PS}_{\mathrm{UDD}_M^T})} - \xi^2_{\mathrm{eff}}}{\xi^2_{\mathrm{eff}}}$ for the corresponding pulse schemes shown in Figure (5).

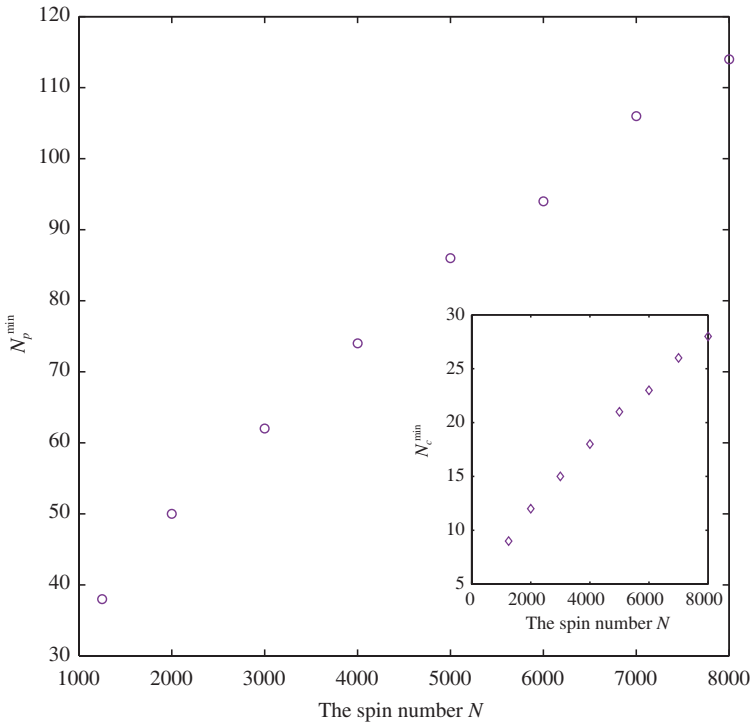

Figure 7 (Color online) The minimum pulse number N_p for different spin number N. The inset shows the corresponding pulse cycle number N_c for different spin number N.

becomes better than that in $\mathrm{PS}_{\mathrm{UDD}_4^T}$ with $N_c = 9$, as presented in Figures 5 and 6.

According to the above analysis, for the system $N = 1250$, our $\mathrm{PS}_{\mathrm{UDD}_4^T}$ has the best performance and requires only $N_p = 38$ ($N_c = 9$) external pulses. In order to determine the optimal M in $\mathrm{PS}_{\mathrm{UDD}_M^T}$ as well as the least pulse number for different spin number N, we also examine the numerical simulations for larger particle number ranging from $N = 2000$ to 8000 as shown in Figure 7. Surprisingly, one can see that the superiority of $\mathrm{PS}_{\mathrm{UDD}_4^T}$ to others is independent of N. More importantly, one can also note that N_p and N_c change with N almost linearly and only $N_p = 114$ pulses are required for 8000 particles, from which one can conclude that $\mathrm{PS}_{\mathrm{UDD}_4^T}$ is optimal for a large range of N.

4 Conclusion

Inspired by UDD theory, we have presented the $\mathrm{PS}_{\mathrm{UDD}_M^T}$ scheme to upgrade the OAT type Hamiltonian to the TACT type. We numerically demonstrate the feasibility of the proposed scheme under current technology. Although the Trotter-Suzuki strategy can tailor the Hamiltonian to the ideal one [25, 27], that strategy typically requires a large number of control pulses to approach high control accuracy. In this work, we show that starting from the OAT type Hamiltonian, the UDD strategy can reach the ideal TACT type of spin squeezing while significantly reducing the number of control pulses. However, in realistic UDD sequences, the Hamiltonian χJ_x^2 can be perfectly achieved, and the other part $-\chi J_y^2$ can only be realized approximately. We find that the best choice is to use BCH second-order approximation to approach $-\chi J_y^2$. This approach can realize the ideal TACT type of spin squeezing and requires fewer control resources. In particular, the $\mathrm{PS}_{\mathrm{UDD}_4^T}$ is best for the $N = 1250$ case, and reduces the pulse number to $N_p = 38$, while it requires $N_p = 100$ for the TS2 scheme. Moreover, we find that the $\mathrm{PS}_{\mathrm{UDD}_4^T}$ is optimal for large-scale N, and the least pulse number N_p changes relative to N almost linearly. In a practical spin squeezing experiment of BEC, unavoidable noise can cause decoherence and hinders the perfect TACT. For example, a stray magnetic field noise commonly occurs [37]. For such type of noise, techniques like spin echo using additional π pulses between neighboring $\mathrm{PS}_{\mathrm{UDD}_4^T}$ pulses can effectively suppress their negative effects. With the current techniques, the proposed scheme has shown great experimental feasibility [34]. We expect that the proposed innovative scheme to generate TACT SSS will advance quantum metrology and quantum information science into new territory.

Acknowledgements This work was supported by National Natural Science Foundation of China (Grant Nos. 11547244, 11547208, 11974334), and the Foundation of Collaborative Innovation Team of Discipline Characteristics of Jianghan University (Grant No. 03100061).

References

1 Kitagawa M, Ueda M. Squeezed spin states. Phys Rev A, 1993, 47: 5138–5143
2 Wineland D J, Bollinger J J, Itano W M, et al. Spin squeezing and reduced quantum noise in spectroscopy. Phys Rev A, 1992, 46: R6797–R6800
3 Wineland D J, Bollinger J J, Itano W M, et al. Squeezed atomic states and projection noise in spectroscopy. Phys Rev A, 1994, 50: 67–88
4 Ma J, Wang X G, Sun C P, et al. Quantum spin squeezing. Phys Rep, 2011, 509: 89–165
5 Bollinger J J, Itano W M, Wineland D J, et al. Optimal frequency measurements with maximally correlated states. Phys Rev A, 1996, 54: R4649–R4652
6 Leibfried D, Barrett M D, Schaetz T, et al. Toward Heisenberg-limited spectroscopy with multiparticle entangled states. Science, 2004, 304: 1476–1478
7 Polzik E S. Quantum physics: the squeeze goes on. Nature, 2008, 453: 45–46
8 Cronin A D, Schmiedmayer J, Pritchard D E. Optics and interferometry with atoms and molecules. Rev Mod Phys, 2009, 81: 1051–1129
9 Appel J, Windpassinger P J, Oblak D, et al. Mesoscopic atomic entanglement for precision measurements beyond the standard quantum limit. Proc Natl Acad Sci USA, 2009, 106: 10960–10965
10 Gross C, Zibold T, Nicklas E, et al. Nonlinear atom interferometer surpasses classical precision limit. Nature, 2010, 464: 1165–1169
11 Riedel M F, Böhi P, Li Y, et al. Atom-chip-based generation of entanglement for quantum metrology. Nature, 2010, 464: 1170–1173
12 Sørensen A, Duan L M, Cirac J I, et al. Many-particle entanglement with Bose-Einstein condensates. Nature, 2001, 409: 63–66
13 Bigelow N. Quantum engineering: squeezing entanglement. Nature, 2001, 409: 27–28
14 Sørensen A S, Mølmer K. Entanglement and extreme spin squeezing. Phys Rev Lett, 2001, 86: 4431–4434
15 Korbicz J K, Cirac J I, Lewenstein M. Spin squeezing inequalities and entanglement of n qubit states. Phys Rev Lett, 2005, 95: 120502
16 Huang H L, Wu D C, Fan D J, et al. Superconducting quantum computing: a review. Sci China Inf Sci, 2020, 63: 180501
17 Amico L, Fazio R, Osterloh A, et al. Entanglement in many-body systems. Rev Mod Phys, 2008, 80: 517–576
18 Xi Q, Wei S H, Yuan C Z, et al. Experimental observation of coherent interaction between laser and erbium ions ensemble doped in fiber at sub 10 mK. Sci China Inf Sci, 2020, 63: 180505
19 Pezzé L, Smerzi A. Entanglement, nonlinear dynamics, and the heisenberg limit. Phys Rev Lett, 2009, 102: 100401
20 Horodecki R, Horodecki P, Horodecki M, et al. Quantum entanglement. Rev Mod Phys, 2009, 81: 865–942
21 Gühne O, Tóth G. Entanglement detection. Phys Rep, 2009, 474: 1–75
22 Lee T E, Chan C K. Dissipative transverse-field ising model: steady-state correlations and spin squeezing. Phys Rev A, 2013, 88: 063811
23 Zhang Y C, Zhou X F, Zhou X X, et al. Cavity-assisted single-mode and two-mode spin-squeezed states via phase-locked atom-photon coupling. Phys Rev Lett, 2017, 118: 083604
24 Su X L, Wang M H, Yan Z H, et al. Quantum network based on non-classical light. Sci China Inf Sci, 2020, 63: 180503
25 Liu Y C, Xu Z F, Jin G R, et al. Spin squeezing: transforming one-axis twisting into two-axis twisting. Phys Rev Lett, 2011, 107: 013601
26 Shen C, Duan L M. Efficient spin squeezing with optimized pulse sequences. Phys Rev A, 2013, 87: 051801
27 Zhang J Y, Zhou X F, Guo G C, et al. Dynamical spin squeezing via a higher-order Trotter-Suzuki approximation. Phys Rev A, 2014, 90: 013604
28 Wu L N, Tey M K, You L. Persistent atomic spin squeezing at the Heisenberg limit. Phys Rev A, 2015, 92: 063610
29 Huang W, Zhang Y L, Zou C L, et al. Two-axis spin squeezing of two-component Bose-Einstein condensates via continuous driving. Phys Rev A, 2015, 91: 043642
30 Chaudhry A Z, Gong J B. Protecting and enhancing spin squeezing via continuous dynamical decoupling. Phys Rev A, 2012, 86: 012311
31 Uhrig G S. Keeping a quantum bit alive by optimized π-pulse sequences. Phys Rev Lett, 2007, 98: 100504
32 Uhrig G S. Erratum: keeping a quantum bit alive by optimized π-pulse sequences. Phys Rev Lett, 2011, 106: 129901
33 Yang W, Wang Z Y, Liu R B. Preserving qubit coherence by dynamical decoupling. Front Phys, 2011, 6: 2–14
34 Edri E, Raz B, Fleurov G, et al. Measuring interactions in a Bose-Einstein condensate using imbalanced dynamical decoupling. 2020. ArXiv:2003.13101v1
35 Micheli A, Jaksch D, Cirac J I, et al. Many-particle entanglement in two-component Bose-Einstein condensates. Phys Rev A, 2003, 67: 013607
36 Tan Q S, Huang Y X, Kuang L M, et al. Dephasing-assisted parameter estimation in the presence of dynamical decoupling. Phys Rev A, 2014, 89: 063604
37 Xu P, Sun H Y, Yi S, et al. Rebuilding of destroyed spin squeezing in noisy environments. Sci Rep, 2017, 7: 14102